Iowa State University
Digital Repository

Retrospective Theses and Dissertations | Iowa State University Capstones, Theses and Dissertations

1-1-2002

The growth of microcrystalline thin films using ECR-PECVD: Silicon and Silicon-Germanium

Yung Moo Huh
Iowa State University

Follow this and additional works at: https://lib.dr.iastate.edu/rtd

Recommended Citation

Huh, Yung Moo, "The growth of microcrystalline thin films using ECR-PECVD: Silicon and Silicon-Germanium" (2002). *Retrospective Theses and Dissertations*. 19882.
https://lib.dr.iastate.edu/rtd/19882

This Thesis is brought to you for free and open access by the Iowa State University Capstones, Theses and Dissertations at Iowa State University Digital Repository. It has been accepted for inclusion in Retrospective Theses and Dissertations by an authorized administrator of Iowa State University Digital Repository. For more information, please contact digirep@iastate.edu.

المنارة للاستشارات

www.manaraa.com

The growth of microcrystalline thin films using ECR-PECVD:

Silicon and Silicon-Germanium

by

Yung Moo Huh

A thesis submitted to the graduate faculty

in partial fulfillment of the requirements for the degree of

MASTER OF SCIENCE

Major: Electrical Engineering

Program of Study Committee:
Vikram L. Dalal (Major Professor)
Robert J. Weber
Douglas K. Finnemore

Iowa State University

Ames, Iowa

2002

المنارة للاستشارات

www.manaraa.com

Graduate College

Iowa State University

This is to certify that the master's thesis of

Yung Moo Huh

has met the thesis requirements of Iowa State University

Signatures have been redacted for privacy

www.manaraa.com

to my better half, Kyu Sung Kim

المنارة للاستشارات
www.manaraa.com

TABLE OF CONTENTS

LIST OF TABLES	v
LIST OF FIGURES	vi
ABSTRACT	vii
CHAPTER 1. INTRODUCTION	1
CHAPTER 2. SAMPLE PREPARATION	6
CHAPTER 3. MATERIALS AND CHARACTERIZATION	12
CHAPTER 4. RESULTS AND DISCUSSION	20
CHAPTER 5. CONCLUSIONS	32
REFERENCES	33
ACKNOWLEDGMENTS	36

المنارة للاستشارات
www.manaraa.com

LIST OF TABLES

Table 1.1 Properties of 'device quality' amorphous silicon films 5

Table 1.2 Properties of 'device quality' microcrystalline silicon films 5

Table 4.1 Deposition parameters for He = 0 sccm group 21

Table 4.2 Deposition parameters for He = 14 sccm group 21

Table 4.3 Deposition parameters for He = 28 sccm group 21

Table 4.4 Properties of He = 0 sccm group 27

Table 4.5 Properties of He = 14 sccm group 27

Table 4.6 Properties of He = 28 sccm group 27

Table 4.7 Deposition parameters for [μc-(Si, Ge):H] films 31

Table 4.8 Properties of [μc-(Si, Ge):H] films 31

المنارة للاستشارات
www.manaraa.com

LIST OF FIGURES

Figure 2.1	ECR-PECVD system in MRC at Iowa State University	8
Figure 3.1	The thickness measurement using Lambda-9	18
Figure 3.2	The measurement of activation energy of dark conductivity	18
Figure 4.1	Deconvolution into two Lorenzian curves. The V_f is the crystalline volume fraction	22
Figure 4.2	Raman spectra of He = 0 sccm. Peaks are off-set for better view	23
Figure 4.3	Raman spectra of He = 14 sccm	25
Figure 4.4	Raman spectra of He = 28 sccm	26
Figure 4.5	Raman spectra for decreasing substrate-temperature	29
Figure 4.6	X-ray diffraction indicates prominent crystalline peaks	30

المنارة للاستشارات

www.manaraa.com

ABSTRACT

A high rate growth method of hydrogenated microcrystalline silicon, μc-Si:H, and silicon-germanium, μc-(Si,Ge):H, has been developed with very low hydrogen dilution ratio on foreign substrates, using a remote electron cyclotron resonance - plasma enhanced chemical vapor deposition (ECR-PECVD) process. In this work, the key variable was the hydrogen dilution, ratio of hydrogen to silane, $[H_2]/[SiH_4]$, which ranged from 3.3 to 10, adding helium systematically. Phase transition from amorphous to microcrystalline states was observed as the amount of added helium was varied. It has been found that hydrogenated microcrystalline silicon films with more than 70 % of crystalline volume fraction were formed at high growth rates of 3.2 Å/sec at low substrate temperature below 300 °C from the mixture of silane and hydrogen with a low hydrogen dilution ratio of as low as 3.3. The addition of helium did not increase the growth rate significantly, but it quickly served as disrupting microcrystalline formation. In addition, the substrate temperature-dependent phase transition was observed. The structural, electrical and optical properties, by Raman shift, x-ray diffraction, dark and photo conductivity, activation energy of dark conductivity, and photosensitivity measurements, were investigated to grow good quality μc-Si:H films at the low hydrogen dilution ratio with high growth rates. The prominent peaks at 520 cm^{-1} from Raman Shift spectroscopy, crystalline peaks from x-ray diffraction pattern, small photosensitivity, and low activation energy of dark conductivity due to grain boundaries in microcrystalline silicon thin films indicated the characteristic of crystalline materials.

للاستشارات المنارة
www.manaraa.com

CHAPTER 1. INTRODUCTION

I. Overview

Silicon thin films have been successfully applied in various electronic devices, such as in thin film transistors (TFT), a switching device in flat panel liquid crystal displays (LCD), image sensors and photovoltaic solar cells, due to higher optical absorption than bulk crystalline silicon and efficient light trapping. The primary attribute of the technology is its large area capability by the plasma chemical vapor deposition (CVD) process on inexpensive substrates, for instance on glass, stainless steel, and plastic polyimide.

Hydrogenated amorphous silicon (a-Si:H) exhibits the full range of semiconducting properties of doping, photoconductivity, and junction formation, although with lower speed and current compared with single crystal silicon from its disordered nature. The plasma deposition technology along with the amorphous structure provide a wide set of compatible materials that allows diversity in device design and considerable band gap engineering.

Hydrogenated microcrystalline silicon (μc-Si:H) thin films have received considerable interest due to their higher mobility and better frequency response than a-Si:H. They also do not suffer from light-induced degradation known for hydrogenated amorphous silicon (a-Si:H) [1]. Structural investigations of μc-Si:H [2, 3] show that the material consists of areas (grains) of perfect crystallinity with an average size of 20 nm forming larger columns parallel to the film growth axis and extending over the entire film thickness. Between theses columns

المنارة للاستشارات
www.manaraa.com

there are disordered regions or internal voids, and the individual small "grains" are separated from each other only by crystalline imperfections like stacking faults.

The definitions for various morphologies of thin film silicon materials are as follows. An amorphous solid is in a non-equilibrium state of a material, which can take a variety of different macroscopic states depending upon the preparative process. It is a single amorphous phase with no feature size at all. Microcrystalline silicon is a mixture of amorphous and crystalline phases. The crystals with typical feature size of less than 20 nm are surrounded with grain boundaries, which are amorphous phase. Both a-Si:H and μc-Si:H have substantially different properties as compared to crystalline silicon. A thin film of hydrogenated silicon contains a large amount of hydrogen, which plays an essential role in the characteristics of such a material.

II. Brief history of amorphous and microcrystalline silicon

N. F. Mott, the Nobel Prize recipient in Physics in 1977 for his work on "The Electron Theory of Disordered Systems", had already started his work on disordered systems in the 1930s with studies of the theory of liquid metals. P. W. Anderson, who shared the Nobel Prize with Mott, made important contribution to the world of amorphous semiconductors through his proposal of the model for localized levels [4].

Sterling and Swann, 1965 were the first to publish the formation of films of "silicon from silane" in a RF glow discharge. Soon after, the first low temperature microcrystalline silicon layers were deposited on glass substrates by Veprek and Marecek in 1968, who used hydrogen plasma and a chemical transport method at 600 °C. The first great breakthrough

المنارة للاستشارات
www.manaraa.com

came with the growth of amorphous silicon from silane (SiH_4) plasma by Chittick et al. in 1969 [5]. They found that plasma-deposited a-Si had better photoconductive properties than that made by the evaporation and sputtering. The second major breakthrough was the 1975 discovery of the possibility of doping the material substitutionally by Spear and LeComber [6]. They demonstrated that the material can be doped n-type and p-type over a large range by adding phosphine (PH_3) or diborane (B_2H_6) to the plasma during growth and it is possible to control the position of the Fermi energy across most of the band gap. Although not clear at first, subsequent work by the Harvard and Chicago groups, showed that the improved properties were the result of hydrogen incorporation into the material [7, 8]. The hydrogen binds to dangling bond defects and removes the corresponding electronic states in the band gap, thus eliminating most of the trapping and recombination centers. Thus electronic-grade amorphous silicon is in fact an alloy of silicon and hydrogen, and was since then called hydrogenated amorphous silicon.

The first a-Si:H field effect transistor, announced in 1978 [9], had a silicon nitride gate dielectric, deposited in the same plasma reactor by combining the gases SiH_4 and NH_3. The plasma nitride was an important innovation, which allowed these thin film transistors (TFT) to be fabricated on glass, at low temperature and with a very high on/off ratio. By this time it was realized that a great variety of silicon alloys could be fabricated by plasma deposition so that an extensive family of materials was available for the technology.

المنارة للاستشارات

www.manaraa.com

III. Physics of hydrogenated amorphous and microcrystalline silicon

The silicon atoms are 4-fold coordinated in a tetrahedral bonding symmetry, but with a significant distribution in bond lengths and bond angles. The 5-10 atomic percent of hydrogen is bonded to the silicon atoms, mostly in the form of Si-H bonds, either isolated or on the surface of small voids. In a-Si:H, free electrons and holes have a scattering length of about interatomic spacing, and consequently a free carrier mobility of only about 1 cm^2/Vs compared to about 100 cm^2/Vs in poly-crystalline silicon. Most importantly, the disorder causes an exponential tail of localized states at the band edges extending into the forbidden gap. The energy dividing the extended and localized states is known as the mobility edge. The mobility gap separating the valence and conduction band mobility edges is approximately the optical band gap. Conduction of both electrons and holes occurs near the mobility edges, but involves frequent trapping and release from these localized states and consequently the effective carrier mobility is further reduced and is also thermally activated. The conduction band tail is narrower than the valence band tail, so that electrons (~1 cm^2/Vs) have a higher mobility than holes (~0.003 cm^2/Vs). Table 1.1 and Table 1.2 [10] show the criteria for 'device quality' amorphous and polycrystalline silicon films, respectively. Silicon-Germanium, (Si, Ge):H, alloys attract special interest due to their tuning ability of optical band gap from 1.0 to 1.7 eV, depending on the Ge content.

المنارة للاستشارات
www.manaraa.com

Table 1.1. Properties of 'device quality' amorphous silicon films.

Property	
AM 1.5 100mW/cm^2 photoconductivity	$1 \times 10^{-5}\ \Omega^{-1}\ cm^{-1}$
Dark conductivity	$1 \times 10^{-10}\ \Omega^{-1}\ cm^{-1}$
Photosensitivity (photo/dark conductivity)	$> 10^5$
Optical band gap	~ 1.7 eV
Activation energy of dark conductivity	~ 0.8 eV
Prominent peaks at Raman Shift	480 cm^{-1}

Table 1.2. Properties of 'device quality' microcrystalline silicon films.

Property	
Orientation of the grains (XRD)	Predominantly (220)
AM 1.5 100mW/cm^2 photoconductivity	$1 \times 10^{-5}\ \Omega^{-1}\ cm^{-1}$
Dark Conductivity	$1 \times 10^{-7}\ \Omega^{-1}\ cm^{-1}$
Photosensitivity (photo/dark conductivity)	$< 10^2$
Band gap, indirect	1.0 - 1.1 eV
Activation energy of dark conductivity	< 0.5 eV
Prominent peaks at Raman Shift	480 cm^{-1} and 520 cm^{-1}

المنارة للاستشارات
www.manaraa.com

CHAPTER 2 SAMPLE PREPARATION

I. Physics of plasma CVD

A *plasma* can be defined as a partially ionized, quasineutral gas. If the very low number of charged particles, ions and electrons, existing in any gas at any temperature is increased by an external source, the electric field due to charge separation can become strong enough to limit particles' own motion and maintain the macroscopic neutrality. This ionized gas is called plasma. The plasma deposition is characterized by the use of non-equilibrium plasma (low-temperature plasma), which forms a non-equilibrium gas phase, which is substantially different from usual thermal CVD method. The electron energy in a plasma is 1-10 eV, which correspondents to 10^4 - 10^5 K in the electron temperature, T_e, the translational temperature, T_{gas}, of the gas molecules (or atoms), ~ 500K, is close to the temperature of the apparatus (the normal temperature), therefore the ratio of T_e to T_{gas} is between 10^2 and 10^3 K. However, because of their large mass, neutrals and ions in the plasma have low energy (a few hundredth of eV). Under these nonequilibrium conditions, the initiation of chemical reactions occurs by collisions with the "hot" electrons. This allows the processing temperature to be much lower than in conventional thermal process using similar chemistry.

The kinetic energy of the electron is responsible for the decomposition of the molecule. By collision with an electron, a molecule is activated to a higher energy state, and its dissociation or ionization then takes place. If B_2H_6 or PH_3 is mixed with the source gas SiH_4

المنارة للاستشارات
www.manaraa.com

in the plasma process, boron or P can be easily doped into a-Si:H, without requiring any diffusion of B or P at higher temperature.

II. Remote ECR-PECVD system at MRC in Iowa State University

Figure 2.1. shows the schematic illustration of the remote electron cyclotron resonance plasma enhanced chemical vapor deposition system at Microelectronics Research Center in Iowa State University. The ECR reactor consists of a two-zone reactor, in which the intense plasma zone is separated from the substrate. The SiH_4 and GeH_4 are excited at a different location from the plasma, which is generated in a carrier gas such as hydrogen and helium by microwave excitation with 2.45 GHz in a remote chamber. The condition of electron cyclotron resonance (ECR) is achieved when the microwave angular frequency ω matches the electron cyclotron frequency, $\omega = eB/m$. Therefore, for a given frequency, the required magnetic field is $B = \omega\, m/e$, which corresponds to 880 G for $\omega/2\pi = 2.45$ GHz. The remote plasma chamber acts as a resonance cavity. The plasma absorbs more than 70 % of the microwave power. The microwave power required to sustain stable plasma is reduced by one-order of magnitude with respect to non-magnetically confined plasma.

The electron density for ECR-CVD is high compared with those of a conventional RF glow discharge. The minimum gas pressure allowing the generation of plasma is much lower under ECR conditions than conventional RF discharge, because the threshold pressure strongly decrease, by almost an order of magnitude, as the magnetic field approaches the ECR condition, since the electrons have a long mean free path as they rotate around the field.

المنارة للاستشارات
www.manaraa.com

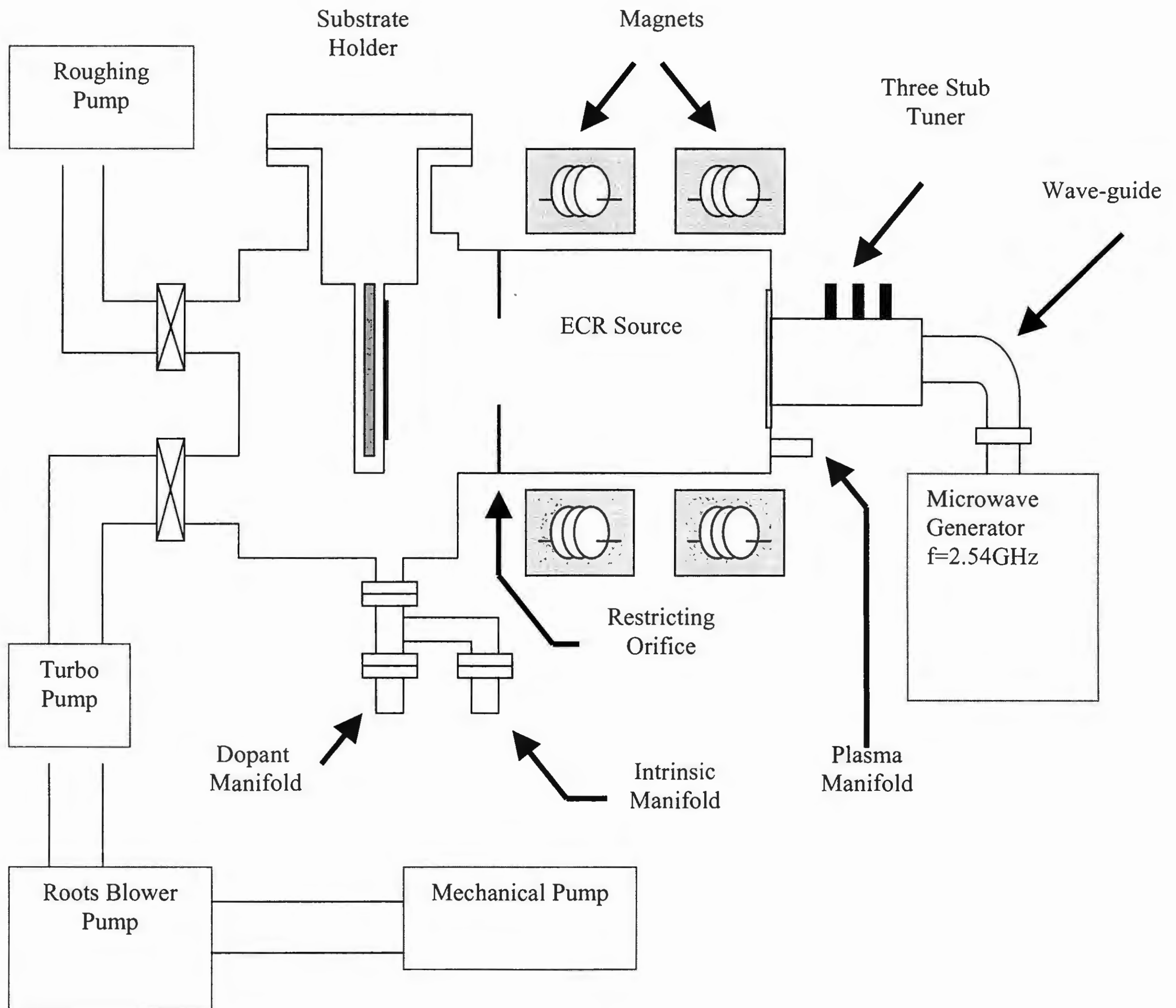

Figure 2.1. ECR-PECVD system in MRC at Iowa State University.

The advantage of the ECR microwave remote plasma CVD compared to conventional glow discharge are (1) the plasma is generated at low pressures, and (2) is remote from the substrate. Low pressure prevents gas phase polymerization and the generation of higher order radicals (such as poly silanes) and the remote plasma zone allows for a good control over ion and radical flux arriving at the substrate. And the other advantages are (3) Efficient energy transfer from the microwave field to the plasma; (4) Easy control of the ion energy by the gas pressure to avoid high-energy particle bombardment of the growing films. Thereby it produces less stress in the film and less damage to the growing surface; (5) Better control of the dissociation of the deposition gas; (6) Reduced powered electrode effects, such as contamination, self-biasing, and hot electron generation; (7) High ionization density; and (8) High plasma density.

III. Experiment

The plasma was generated in the remote chamber from substrate by microwave excitation at 2.54 GHz through a quartz window. A rectangular waveguide system was used to transport the microwaves to the chamber. The system has three tuners to tune the polarization of the microwaves. The ECR condition was established with the use of two external magnetic coils. By adjusting the magnetic field strength of each coil, the position and strength of ECR region within the plasma generation region can be controlled. Two DC power supplies are used to power the coils. The reflected power from the substrate was set to be slightly above the minimum value possible. This setting corresponds to a maximum power transfer from the source to plasma and again to substrate, as well as stable magnetic field at

المنارة للاستشارات

www.manaraa.com

the position of active plasma. The restricting orifice, which divides ECR chamber and deposition chamber, provides uniformity and diverging cone shape of the plasma entering the deposition chamber. The substrate holder uses a stainless steel mask to hold the substrate in place. Typical substrate sizes are 2×2 in^2. Throughout this research, 7059 corning glasses are used for substrates. The substrate holder is externally attached to a heating block, which can control the substrate temperature up to 800 °C. The process chambers are evacuated by the turbopump down to 10^{-6} to 10^{-7} Torr before the deposition. The turbopump is backed by the roots blower pump and mechanical pump and the valves are open only after a separately located roughing pump brings the pressure down to ~1 mTorr from atmospheric pressure. All pump systems are constantly purged with nitrogen to prevent building up of any residual toxic gases. There are three separate feedstock lines for plasma, intrinsic and dopant manifolds. Plasma gases of hydrogen and helium are introduced in the far end of the plasma source chamber. Plasma is generated by microwave excitation. The process gases, such as silane and germane, are flowed into the deposition chamber near the substrate. These gases are then ionized and dissociated into radicals due to the electrons with high energy by external magnetic field.

The substrates are prepared by boiling in acetone for 10 minutes, followed by 10 minutes of boiling in methanol. They are, then, stored in clean methanol. The substrate is blown dry with nitrogen just before being loaded. More than ten times of purging cycles is followed with nitrogen, plasma gas and deposition gas subsequently right after loading new substrate to remove any remnant moisture and oxygen gas. In between purges, the substrate heater is turned on and temperature is set about 50 °C higher than the desired deposition temperature to ensure full outgasing from the substrate. Following the purges, a shutter is

المنارة للاستشارات
www.manaraa.com

placed in front of the substrate for the chamber etching and dummy layer growth. He plasma is used for etching and growth of dummy layer on the chamber wall. The pressure is set to be 15 mTorr. This step is to remove any impurities that might be deposited from the previous experiment. Silane gas flows into chamber for etching as well as coating fresh dummy layer around the chamber. Microwave power is set at 150 W for these procedures. The deposition pressure for target material in this research is set between 5 and 10 mTorr. Microwave power was set at 200 W during film deposition. Upon completion of the deposition, the film is left to cool down to below 100 °C before being pulled out. While cooling, the chamber is back filled with 1 Torr of hydrogen and silane to prevent oxidation.

المنارة للاستشارات

www.manaraa.com

CHAPTER 3 MATERIALS AND CHARACTERIZTION

I. Growth mechanism of hydrogenated silicon thin films

The silane is introduced at a location near the substrate. As the magnetic field diverges into the deposition chamber, an electric field is generated in the plasma column, and ionized radicals (SiH_n^+) from the plasma are driven to the substrate where they bombard the growing surface. A large ion flux with a sufficiently low energy enhances the deposition rate while material quality is preserved. The large ion flux allows the use of a low substrate temperature. The ion energy can be controlled by the gas pressure.

In the ECR-PECVD system, there are several reactions near the surface of substrate:

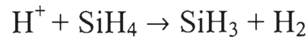

$$H^+ + SiH_4 \rightarrow SiH_3 + H_2$$

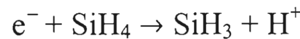

$$e^- + SiH_4 \rightarrow SiH_3 + H^+$$

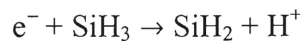

$$e^- + SiH_3 \rightarrow SiH_2 + H^+$$

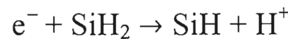

$$e^- + SiH_2 \rightarrow SiH + H^+$$

This dissociation occurs in the same way as in GeH_4. It is believed that SiH_3 and GeH_3 are dominant and the most important radicals, due to their higher surface mobility and low sticky coefficient. If other radicals become dominant during deposition, the surface will be rough and many dangling bonds and microvoids will be formed [11].

The standard model of hydrogen silicon growth by Matsuda, Gallagher and Perrin (MGP model) [12, 13, 14] showed that the growth of hydrogenated silicon film is limited

www.manaraa.com

primarily by surface diffusion of SiH_3 radical. The dangling bonds at the surface of a-Si:H are almost all bonded with H, with only an occasional bond being open to insertion by a silyl (SiH_3) radical. When adjacent surface sites have silyl radicals bonded into them, the wing-bonded H atoms on adjacent sites self react, giving rise to H_2, and then eliminated from surface. This is possible because the bond energy of H_2 is higher than the bond energy of Si-H. The resulting adjacent Si dangling bonds then react to create a Si lattice with a surface bonded H. This theory was improved later by Dalal and coworkers [15], who suggested that the primary consideration which determines the growth of hydrogenated silicon films is not surface diffusion, but rather the removal of surface hydrogen, and this elimination takes place not by reactions between neighboring H bonded to adjacent Si atoms, but rather by extraction of hydrogen by H radicals and inert gas ions. A high H dilution leads to a significant concentration of H ions and radicals impinging on the surface, and these remove the bonded H. The H ions also penetrate deeper into the lattice, and remove some more bulk H ions. The role of inert gas ions, such as Ar and He is to break the surface H bonds, thereby creating a dangling bond, and allowing another silyl radical to insert itself. The inert gas ions do not penetrate deep into the substrate, but H ions do. If the surface hydrogen is not removed, then the bonded Si-H structures get buried, new material grows around it, and a microstructure with a significant void concentration and clustered Si-H bonds form in the lattice. Such microstructure then leads to rapid degradation. Bombardment by inert gas ions can enhance the elimination of excess H at the surface, thereby reducing the probability of forming microvoids in the films. High ion flux densities are beneficial, but high energies, inexcess of ~10 eV or so may damage the material. We only need a few eV ions (~3 eV) to break the Si-H bonds at the surface [16].

المنارة للاستشارات
www.manaraa.com

II. The phase diagram of hydrogenated microcrystalline silicon films

The role of H dilution is complex. It removes H from the surface and subsurface, enhances radical selectivity by increasing the fraction of silyl radicals in the growth process [17], and is also involved in subsurface bond reconstruction (Etching). H ions can convert a-Si into microcrystalline Si [18]. In contrast, when H ions are not present, or the ion energy is low (<1 eV), the material is highly defective, and a very high temperature (~450 °C) must be used to obtain satisfactory properties. H ions with enough energy (>2-3 eV) to break the surface-bonded H and penetrate the lattice to homogenize and improve the microstructure by removing weakly bonded H, are essential for promoting the growth of better materials.

It is generally accepted in μc-Si:H community that the amorphous-to-microcrystalline silicon transition is favored in highly H diluted silane discharge at high power density or in sequential alternative discharges of SiH_4 and H_2 gases [19, 20]. When μc-Si:H is deposited on noncrystalline substrates at low substrate temperature (< 500°C) the layer usually grows amorphous at first and a so-called incubation layer is formed, in which the crystallites start to nucleate [21]. As the deposition goes on, the silicon crystallites enlarge and aggregate until the transition is complete [22]. Depending on the deposition conditions the thickness of the transition layer ranges from several nanometers up to a few hundred nanometers [23].

The electronic defects are supposed to be concentrated at boundaries between the crystalline grains [24]. Seto introduced the grain boundary-trapping model [25], where in polycrystalline silicon the transport properties are governed by carrier trapping at the boundaries, leading to the creation of potential energy barriers, which impede the motion of carriers between grains. However, in relatively small grains of about 10nm, the number of

المنارة للاستشارات
www.manaraa.com

free carriers is not sufficient to completely fill the grain boundary defects and build up the barriers at the grain boundaries [26, 27]. Yet many impurities, in particular oxygen contamination [28], can introduce additional carriers and give rise to grain boundary barriers. On the other hand, the grain boundaries can be passivated by a high concentration of hydrogen [29].

Among the most important contributions for the understanding of the physical and chemical processes in the plasma deposition of the μc-Si:H materials have been the work of Veprek, who was the first to recognize that the low-pressure plasma deposition is in fact the result of a competition between "deposition" and "etching" by the reactive species in the plasma [30]. For a gas flow of almost pure silane in low-pressure plasma, the dominant process is the deposition if silicon hydrides that produce a film of hydrogenated amorphous silicon, as the small concentration of active radicals in the plasma provides a negligible etching of the surface. Veprek showed that when the rate of etching, mostly due to the large amount of hydrogen, becomes of the same order as that of the deposition of silicon, it is favorable for the formation of the crystalline silicon films. High rate of chemical exchange between the solid and the plasma will yield a quasi-equilibrium situation that will facilitate the formation of the thermodynamically stable material.

Recently, there have been serious discussions on the existence of phase transition from amorphous to microcrystalline phases in the functions of hydrogen dilution to silane ([H_2/SiH_4]). The high dilution of silane with hydrogen was found to enhance the crystallization of PECVD Si films [31]. Therefore, hydrogen atoms are believed to promote surface coverage effect, the etching reaction, and/or the modification of the Si-Si network. The use of highly diluted silane also gives rise to a high hydrogen atom flux toward the

المنارة للاستشارات
www.manaraa.com

surfaces and also that it favors the production of silyl (SiH_3) radicals that are supposed to be the main film precursor [32]. Fujiwara and coworkers showed that a μc-Si:H nuclei density increases significantly as the hydrogen dilution ratio to silane increases [33].

One of the most important results from highly diluted hydrogen in plasma is the effective etching mechanism. Therefore, it becomes general agreement that removal of hydrogen from the growth surface during growth of silicon film is the key factor to observe the transition from amorphous to microcrystalline phases. The consensus in the community is that μc-Si:H films are to be deposited under the condition of $[H_2/SiH_4] > 100$ [34]. The most recent comprehensive study by J. Koh on the phase diagram of μc-Si:H shows that , to ensure crystalline volume fraction of above 70 %, it is required at least to have $[H_2/SiH_4] > 40$ [35].

The questions to be answered are as follows. (1) What is the minimum amount of hydrogen dilution to have phase transition from amorphous to microcrystalline silicon films of about 1μm thickness? (2) What is the effect of adding He ions, possessing energies of ~ 10 eV, to phase transition and (3) to growth rates? (4) Is there any substrate temperature-dependent phase transition? (5) What would it be the growth rate for μc-Si:H grown by ECR-PECVD? Theses questions are the primary motivations throughout this investigation.

III. Characterization of hydrogenated microcrystalline silicon films

The Raman Shift spectra, x-ray diffraction, photo- and dark- conductivity, and activation energy of dark conductivity measurements were conducted to investigate microcrystalline characteristics of plasma deposited silicon films. The thickness *t* of films are obtained from the measurements of transmission scan in the wavelength range of 1000 to

المنارة للاستشارات
www.manaraa.com

2500 nm using Lambda-9 spectrophotometer as shown in Figure 3.1. The relationship to calculate the thickness is $t = 1/ [2 n (1/\lambda_1 - 1/\lambda_2)]$, where n is index of reflection and λs are wavelengths of adjacent peaks. Conductivity measurements provide the early insight to the structural and electrical qualities. The photoconductivity is measured under illumination of 1.5 AMS lamp with a spectrum similar to the Sun. A 100 V is applied across the film and the current is measured. The conductivities are given by σ = (I/V) (W/Lt), where W/L is the ratio of width to length at contact points, and t is the thickness of film. The characteristic of microcrystalline silicon is its higher dark conductivity than amorphous silicon. Amorphous silicon will have dark conductivities of between 10^{-9} to 10^{-11} Ω^{-1} cm^{-1}, while microcrystalline silicon will have in the 10^{-3} to 10^{-5} Ω^{-1} cm^{-1}. The photosensitiviy is the ratio of photoconductivity to dark conductivity. The good quality amorphous silicon will have photosensitivity more than 10^5, while good quality microcrystalline silicon film will have less than 10^2. Prior to the temperature-dependent conductivity measurements the films are annealed at 200 °C for at least 1 hour followed by quenching to room temperature. Then the dark conductivity was measured as the films was cooled with a rate dT/dt = 10 K/10 min. In Figure 3.2., for the temperature range between 200 °C and 100 °C, Arrhenius plots of dark conductivity shows activated behavior $\sigma = \sigma_0 \exp(-E_A/kT)$, with an activation energy of E_A. For amorphous silicon film, the activation energy is ~ 0.8 eV and it is roughly a half of the cubic band gap. It is expected to have less than 0.5 eV of activation energy for the microcrystalline with grain boundaries.

X-ray peaks are measured using Cu Kα line (λ=1.542 Å) with step size of 0.05° of 2θ. Microcrystalline silicon film will show prominent peaks from the (111), (220), and (311) planes at 28.1°, 47.2°, and 55.5°, respectively. The average grain size in the microcrystalline

المنارة للاستشارات
www.manaraa.com

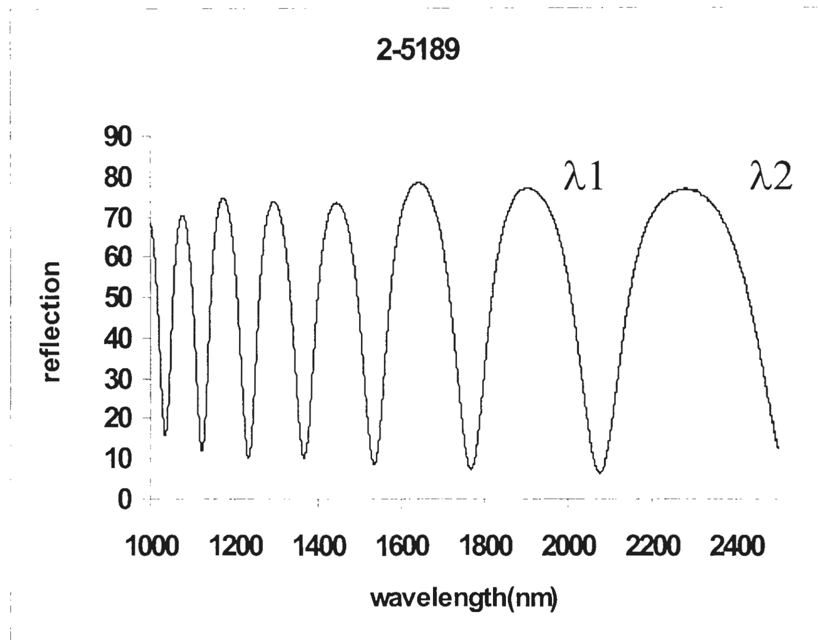

Figure 3.1. The thickness measurement using Lambda-9.

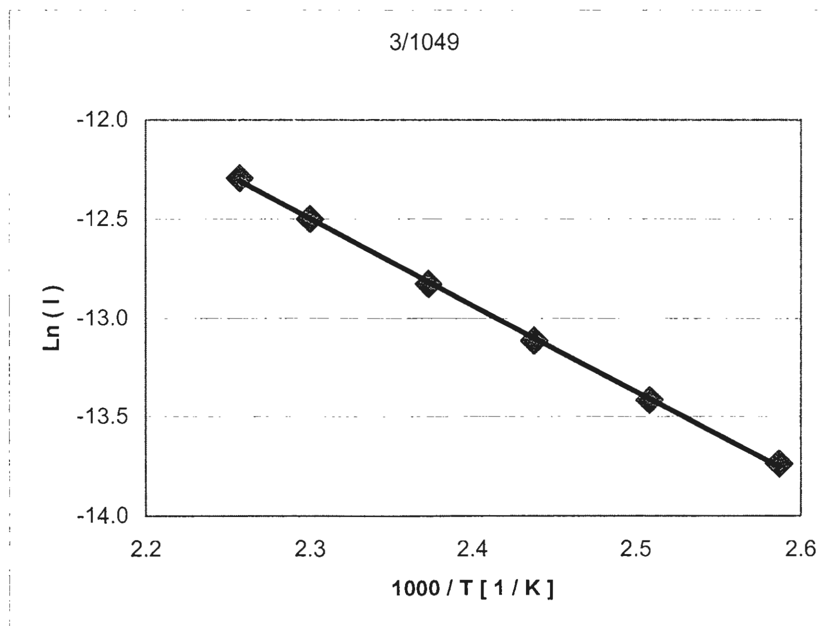

Figure 3.2. The measurement of activation energy of dark conductivity.

المنارة للاستشارات
www.manaraa.com

films can be estimated using Scherrer's formula, $x = 0.94\ \lambda/(B_{2\theta}\ \cos\theta_B)$, where $B_{2\theta}$ is fullwidth in radians at Half maximum intensity, if film is thick enough compared to the wavelength of the x-ray. The Raman spectroscopy measures energy shift of the emitted light from the incoming light energy by either gaining or losing energy by interacting with phonons and it is the best method to determine the phases present in silicon films. Raman Shift spectra (Nd:YAG Laser with λ=1064 nm) have been used to measure the structure changes of the films, in which the peaks at 520 cm^{-1} are associated with the transverse optical (TO) mode of crystal silicon, whereas signals of the amorphous silicon with grain boundaries appear between 480 cm^{-1} and 520cm^{-2} [36]. The crystalline volume fraction V_f, is defined from the deconvoluted intensities I_c and I_a of the Raman spectra, at 520 cm^{-1} and 480 - 520cm^{-2}, respectively, by applying $V_f = I_c / (I_c + I_a)$.

المنارة للاستشارات

www.manaraa.com

CHAPTER 4 RESULTS AND DISCUSSION

A set of thirteen films were prepared to investigate; firstly, the effect of hydrogen dilution as the ratio of hydrogen to silane varies from 10 to 3.3, and secondly, the effect of adding He ion systematically to plasma. Deposition time (60 min), substrate temperature (350 °C), deposition pressure (5 mTorr), and microwave power (200 W) were set constant. Samples were divided into three groups and labeled as He = 0 sccm, He = 14 sccm, and He = 28 sccm groups. The deposition parameters are shown in Table 4.1, 4.2 and 4.3, respectively.

Figure 4.1. shows a typical Raman Shift spectra. Intensity in arbitrary unit vs. Raman Shift is plotted in a range within 440 and 600 cm^{-1} to identify a crystalline peak and a peak from amorphous silicon with grain boundaries. Crystalline volume fraction is derived from $V_f = I_c/(I_c+I_a)$, where I_c and I_a are peak intensities from crystalline and amorphous, respectively.

In Figure 4.2, Raman spectra of the group of He = 0 sccm are plotted. Peaks are off-set along x-axis for better view. It is clear that microcrystalline silicon formed from the peak at 520 cm^{-1} and broad shoulders near 480 cm^{-1} indicate that mixed phases are present in these films. The activation energies are added for comparison with the Raman result. The low activation energy confirms that it is microcrystalline silicon film. There is no indication of abrupt change as hydrogen dilution decreases from 10 down to 3.3. This is the main result in this research, i.e., microcrystalline phase can be formed with hydrogen dilution as low as 3.3.

المنارة للاستشارات
www.manaraa.com

Table 4.1. Deposition parameters for He = 0 sccm group.

Sample #	H_2 [sccm]	He [sccm]	SiH_4 [sccm]	H_2 / SiH_4
980	20	**0**	6	3.3
981	30	**0**	6	5.0
982	40	**0**	6	6.7
983	50	**0**	6	8.3
984	60	**0**	6	10.0

Table 4.2. Deposition parameters for He = 14 sccm group.

Sample #	H_2 [sccm]	He [sccm]	SiH_4 [sccm]	H_2 / SiH_4
985	20	**14**	6	3.3
986	30	**14**	6	5.0
988	40	**14**	6	6.7
989	50	**14**	6	8.3
990	60	**14**	6	10.0

Table 4.3. Deposition parameters for He = 28 sccm group.

Sample #	H_2 [sccm]	He [sccm]	SiH_4 [sccm]	H_2 / SiH_4
992	20	**28**	6	3.3
994	30	**28**	6	5.0
993	40	**28**	6	6.7

المنارة للاستشارات
www.manaraa.com

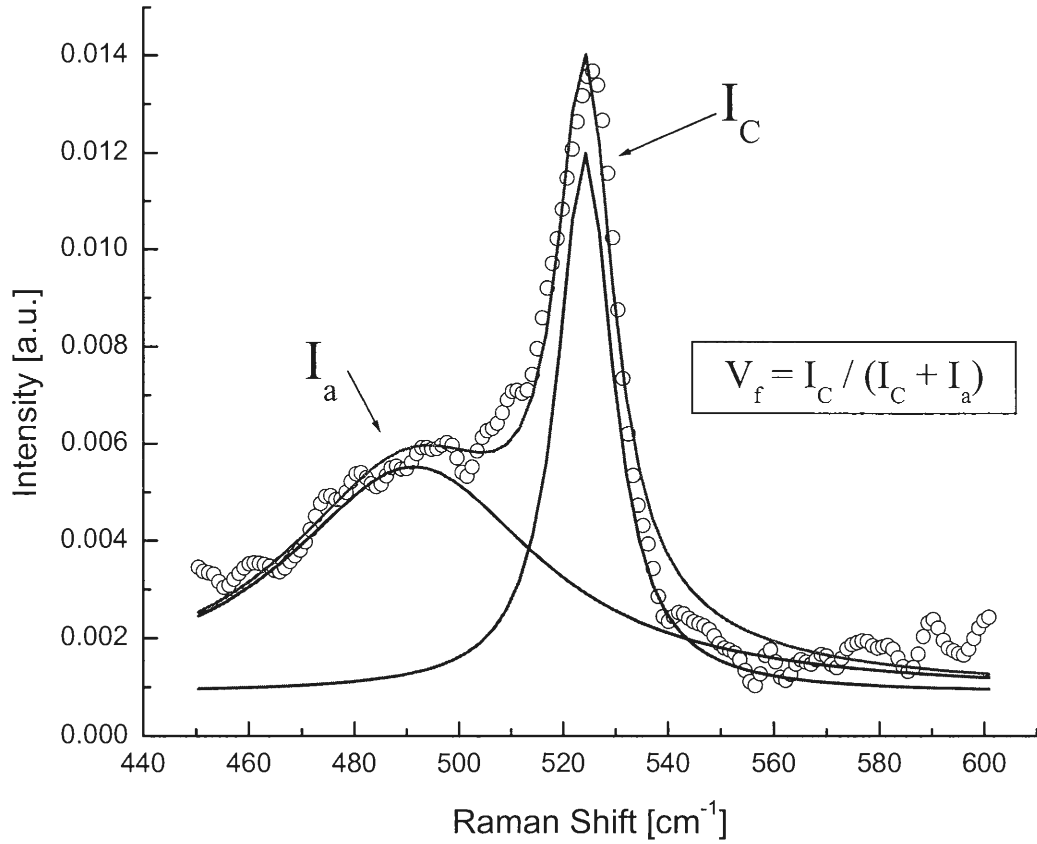

Figure 4.1. Deconvolution into two Lorenzian curves. The V_f is crystalline volume fraction.

المنارة للاستشارات
www.manaraa.com

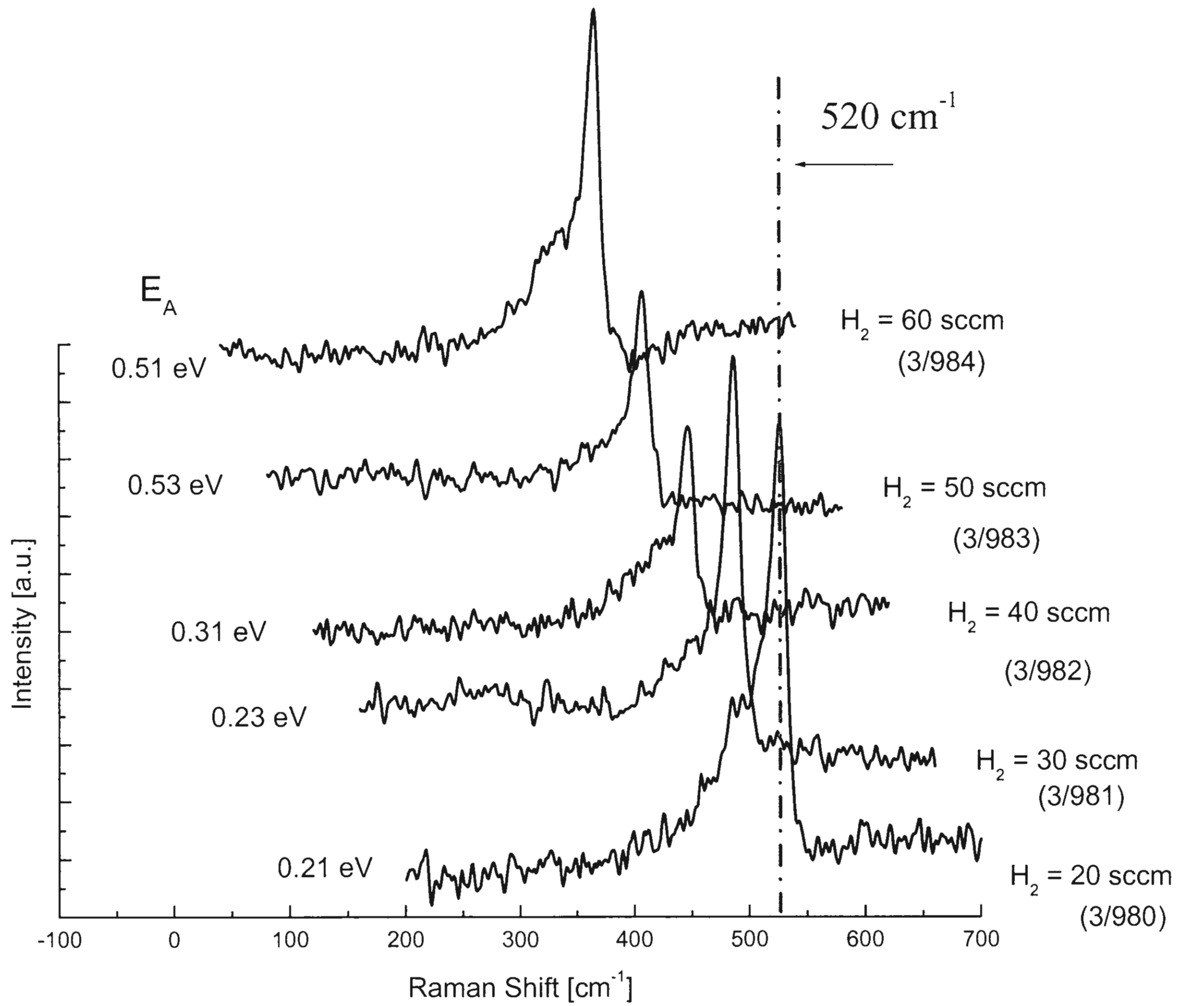

Figure 4.2 Raman spectra of He = 0 sccm. Peaks are off-set for better view.

المنارة للاستشارات
www.manaraa.com

To investigate the effect of adding inert ion into plasma, helium is added systematically. Figure 4.3 and Figure4.4 are Raman Shift spectra plots of He = 14 sccm and He = 28 sccm groups, respectively. Activation energy hiked up as microcrystalline phase faded away as a result of He addition in a gradual manner.

Two important results were obtained by adding helium. First, films grown with higher hydrogen dilution failed to make transition to microcrystalline phase. Second, as the flow rate of helium doubled, microcrystalline phase stopped forming more quickly as hydrogen dilution decreased. However, microcrystalline phase was still formed for low hydrogen dilution, although microcrystalline phase for highly diluted hydrogen samples disappeared readily. This is quite interesting because this means that helium ion in plasma, with energy of ~10 eV, is too energetic for microcrystalline formation. Bombardment of He ions on the growth surface would destroy the thermodynamically equilibrium state, which is a necessary stage for the formation of microcrystalline phase. Furthermore, the deposition growth rate was not significantly affected by adding helium. For example, films grown with 20 sccm of hydrogen for three groups resulted in the growth rate of 3.24, 3.36, and 3.38 Å/sec, respectively. This indicates that the growth mechanism of amorphous and microcrystalline phases is quite different from each other. In amorphous silicon growth, adding helium gives rise to higher growth rate. The growth of microcrystalline phase involves very slow chemical mechanism. There must be present a certain amount of hydrogen for subsurface etching mechanism to remove microvoids and to passivate dangling Si bonds and growth surface requires to maintain an equilibrium state for transition to microcrystalline phase. Table 4.4, 4.5, and 4.6 is lists of film thickness, growth rate, photosensitivity, activation energy, identification of microcrystallinity and volume fraction from Raman Shift spectra.

المنارة للاستشارات
www.manaraa.com

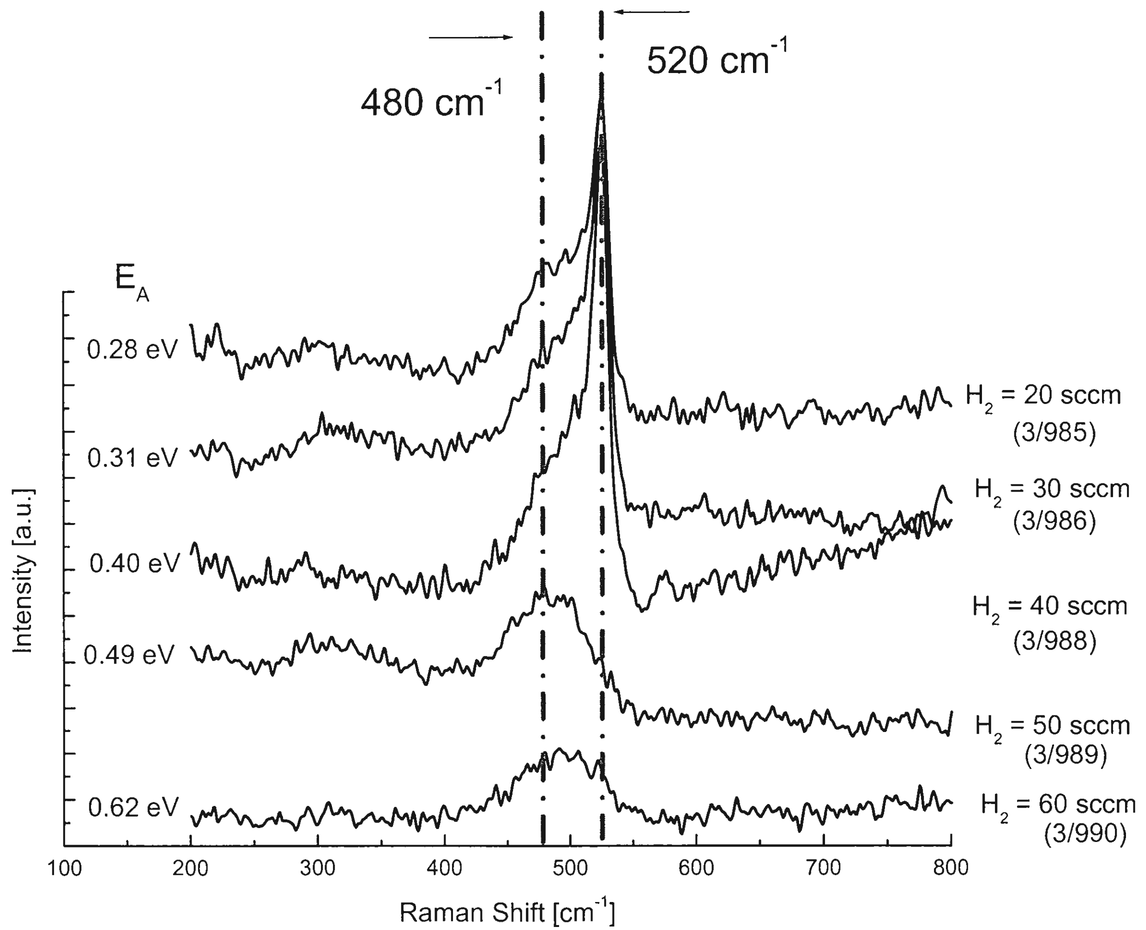

Figure 4.3. Raman spectra of He = 14 sccm.

www.manaraa.com

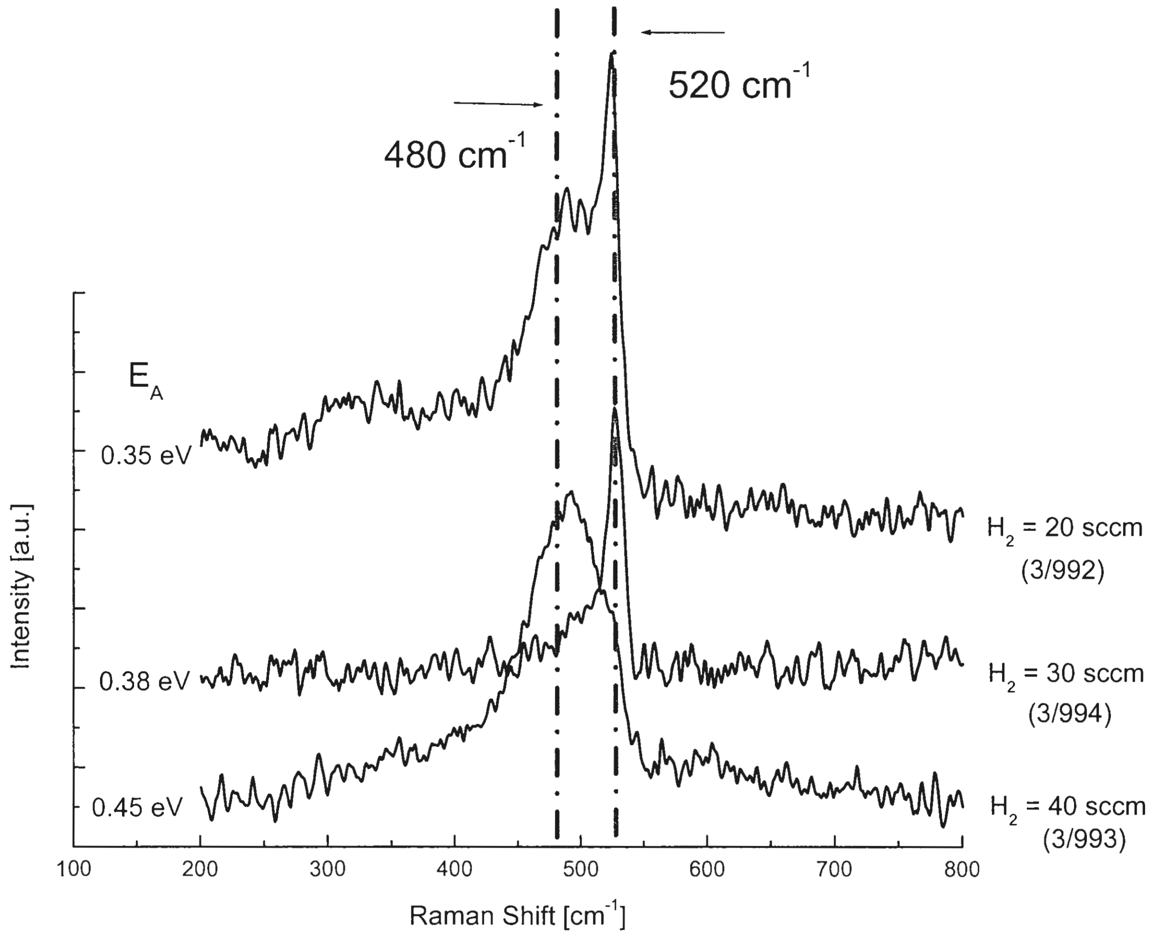

Figure 4.4. Raman spectra for He = 28 sccm.

www.manaraa.com

Table 4.4. Properties of He = 0 sccm group.

Sample #	t [μm]	rate [Å/sec]	Photosensitivity	E_A [eV]	μc- / a-	V_f
980	1.17	3.2	1.26×10^0	0.21	**μc-Si:H**	0.69
981	1.09	3.0	1.18×10^0	0.23	**μc-Si:H**	0.74
982	1.02	2.8	1.70×10^0	0.31	**μc-Si:H**	0.71
983	0.91	2.5	1.46×10^0	0.53	**μc-Si:H**	0.72
984	1.36	3.8	2.34×10^0	0.51	**μc-Si:H**	0.71

Table 4.5. Properties of He = 14 sccm group.

Sample #	t [μm]	rate [Å/sec]	Photosensitivity	E_A [eV]	μc- / a-	V_f
985	1.21	3.4	2.28×10^0	0.28	**μc-Si:H**	0.58
986	1.06	2.9	2.85×10^0	0.31	**μc-Si:H**	0.62
988	1.29	3.6	2.07×10^0	0.40	**μc-Si:H**	0.69
989	1.22	3.4	1.72×10^1	0.49	a-Si:H	0
990	1.01	2.8	1.96×10^2	0.62	a-Si:H	0

Table 4.6. Properties of He = 28 sccm group.

Sample #	t [μm]	rate [Å/sec]	Photosensitivity	E_A [eV]	μc- / a-	V_f
992	1.22	3.4	3.73×10^0	0.35	**μc-Si:H**	0.49
994	1.00	2.8	6.91×10^0	0.38	**μc-Si:H**	0.83
993	1.25	3.5	2.50×10^0	0.45	a-Si:H	0

المنارة للاستشارات
www.manaraa.com

Next, a set of six samples was prepared to study the substrate temperature effect. This samples were pre deposited with amorphous silicon layers for ten minutes in order to monitor the effect of having precursor of nucleation site. Ten minutes of amorphous layer was pre-deposited with 21 sccm of helium and 2.2 sccm silane and no hydrogen plasma gas under the pressure of 15 mTorr. For the purpose of comparison of the pre-amorphous layer deposition, a sample was prepared in the exactly same environment except this sample didn't have a pre-deposited amorphous layer. Sample #1050 is the one with pre-deposited amorphous layer and sample #1055 is the counter part. Surprisingly, there is no evidence observed in this experiment showing any improvement in the growth of microcrystalline layer with pre-deposited amorphous layer. No decisive conclusion could be drawn from this. Both turned out to have mixed phases and crystalline volume fraction is about 70 %. The other purpose of this set of experiment is to investigate the transition to microcrystalline phase as substrate temperature decreased down to 275 °C. The deposition parameter and properties of films are listed in Table 4.7 and 4.8, respectively. It was observed that as substrate temperature was set at 275 °C, there was no microcrystalline peak found. The Raman Shift spectra is plotted in Figure 4.5.

To confirm the presence of microcrystalline phase in films, x-ray diffraction (XRD) was measured. Figure 4.6 indicates prominent crystalline peaks at 28.1°, 47.2°, and 55. 5° of 2θ, which correspond to (111), (220), and (311) planes. To extract background from 7059 glass substrate, XRD result from glass is plotted along with the film from each group. The average grain size in the microcrystalline films was determined by x-ray diffraction to be in the nanometer range. But due to the thin film thickness (~1 μm) comparing to the penetration depth of x-ray, grain size extraction is not meaningful with these samples.

المنارة للاستشارات
www.manaraa.com

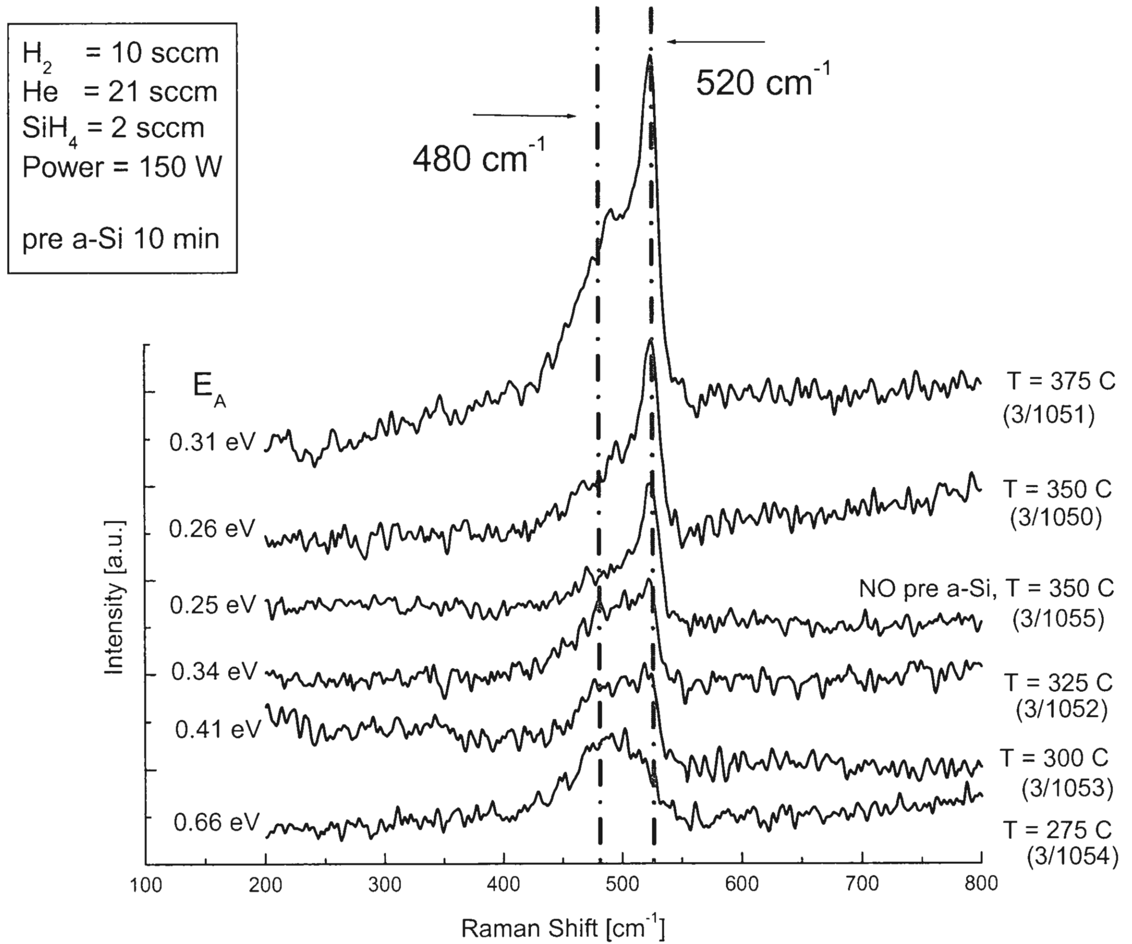

Figure 4.5 Raman spectra for decreasing substrate-temperature.

www.manaraa.com

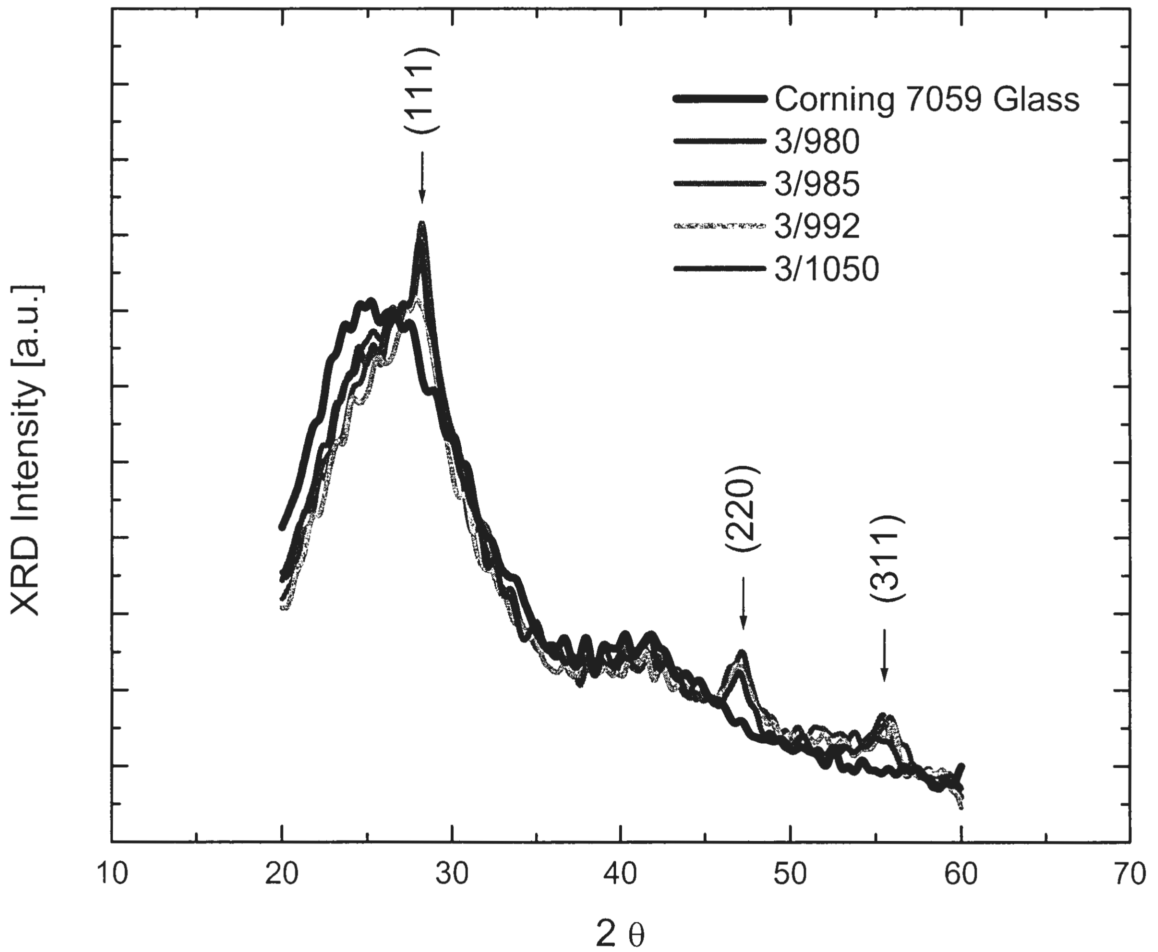

Figure 4.6 X-ray diffraction indicates prominent crystalline peaks.

المنارة للاستشارات
www.manaraa.com

Finally, hydrogenated microcrystalline silicon-germanium films [μc-(Si, Ge):H] were deposited under the guideline of deposition of μc-Si:H films. The evidence of formation of microcrystalline phase came from the measurements of activation measurements and photosensitivity. The deposition parameters and material properties are listed in Table 4.7 and 4.8, respectively.

Table 4.7. Deposition parameters for [μc-(Si, Ge):H] films.

Sample #	P [mTorr]	H_2 [sccm]	He [sccm]	SiH_4 [sccm]	GeH_4 [sccm]	$H_2/(SiH_4+GeH_4)$
1118	5	30	0	2	2	7.5
1122	10	40	0	2.3	2.3	8.7
1123	10	40	7	2.3	2.3	8.7
1125	10	20	7	2.3	2.3	4.4

Table 4.8. Properties of [μc-(Si, Ge):H] films.

Sample #	t [μm]	rate [Å/sec]	Photosensitivity	E_A [eV]
1118	0.782	2.17	1.19×10^0	0.23
1122	0.692	1.92	1.11×10^0	0.18
1123	0.712	1.98	1.13×10^0	0.19
1125	0.768	2.13	1.15×10^0	0.20

المنارة للاستشارات
www.manaraa.com

CHAPTER 5 CONCLUSIONS

Using a remote electron cyclotron resonance - plasma enhanced chemical vapor deposition (ECR-PECVD) process, thin films of hydrogenated microcrystalline silicon, μc-Si:H, and silicon-germanium, μc-(Si,Ge):H, have been deposited. The key variable in this work is the hydrogen dilution ratio to silane. It was found, through extensive film growth, that the low hydrogen dilution does lead to the deposition of microcrystalline silicon materials on foreign substrate at high growth rate with over 70% of crystalline volume fraction. High quality μc-Si:H thin film can be grown with dilution ratio of as low as 3.3. This is very contradictory to the previously accepted growth mechanism of microcrystalline phase, where it was regarded that the hydrogen dilution ratio should be more than 30 to grow microcrystalline phase. The addition of helium did not increase the growth rate significantly, but it quickly served as disrupting microcrystalline formation. This indicates the growth mechanism of microcrystalline phase is required to have quasi-equilibrium state during growth and it is quite different from that of amorphous phase. In addition, the substrate temperature-dependent phase transition was also observed. For ECR-PECVD system in MRC, the minimal substrate temperature is about 300 °C to grow microcrystalline materials with high microcrystalline volume fraction.

المنارة للاستشارات
www.manaraa.com

REFERENCES

1. S. Veprek and V. Marecek, Solid-State Electron. **11**, 683 (1968).

2. M. Luysberg, P. Hapke, R. Carius, and F. Finger, Philos. Mag. A **75**, 31 (1997).

3. L. Houben, M. Luysberg, P. Hapke, R. Carius, F. Finger, and H. Wagner, Philos. Mag. A **77**, 1447 (1998).

4. P. W. Anderson, Phys. Rev. Lett. **34**, 953 (1975).

5. R. C. Chittick, J. H. Alexander and H. F. Sterling, J. Electrochem. Soc. 115, **77** (1969).

6. W. E. Spear and P. G. LeComber, Solid State Commun. **17**, 1193 (1975).

7. A. J. Lewis, G. A. N. Connell, W. Paul, W. Pawlik and R. Temkin, AIP Conf. Proc. **20**, 27 (1974).

8. H. Fritzsche, Proc. 7th. Int. Conf. On Amorphous and Liquid Semiconductors, (CICL, Edingburg), 3 (1977).

9. A. J. Snell, K. D. Mackenzie, W. E. Spear, P. G. LeComber and A. J. Hughes, Appl. Phys. 24, 347 (1981)).

10. R. E. I. Schropp and M. Zeman, "Amorphous and Microcrystalline Silicon Solar Cells", Kluwer Academic publishers, Dordrecht, (1998)

11. W. Luft and Y. Tsuo, "Hydrogenated Amorphous Silicon Alloy Deposition Process", Marcel Dekker, Inc. New York (1993).

المنارة للاستشارات
www.manaraa.com

12. J. R. Doyle, D. Doughty and A. Gallagher, J. Appl. Phys., **68**, 4375 (1990)

13. A. Matsuda and K. Tanaka, J. Non-Cryst. Solids, **97-98**, 1367 (1987)

14. J. Perrin, in " Plasma Deposition of a-Si materials", Ed. G. Brunno, P. Capezzuto and A. Madan (Academic, San Diago, 1995), **79** (2000)

15. V. L. Dalal, T. Maxson, and S. Haroon, "Influence of Plasma Chemistry on the Properties of Amorphous (Si, Ge) Alloy Devices", Mat. Res. Soc. Symp. Proc., **507**, 441 (1998)

16. V. L. Dalal, " Growth Chemistry of Amorphous Silicon and Amorphous Silicon-Germanium Alloys", not published.

17. V. L. Dalal, S. Kaushal, T. Maxson, R. Girvan, A. Boerner, Proc. Am. Inst. Phys. **394** 33. (1997).

18. (a) Y. Okazaki et al., J. Non-Cryst. Solids **266-269**, 54 (2000) (b) S. Miyazaki, N. Fukhara, M. Hirose, J. Non-Cryst. Solids **266-269**, 59 (2000)

19. A. Asano, Appl. Phys. Lett. **56**, 533 (1990)

20. M. Otobe and S. Oda, Jpn. J. Appl. Phys. **31**, L1443 (1992)

21. S. Hamma and P. R. I Cabarrocas, J. Appl. Phys. **81**, 7282 (1997)

22. H. Fujiwara, M. Kondo, and A. Matsuda, Phys. Rev. B **63**, 115306 (2001)

23. S. Koynov et al., J. Non-Crys. Solids **198-200**, 1012 (1996)

24. P. G. L. Comber, G. Willeke, and W. E. Spear, J. Non-Cryst. Solids **59-60**, 795 (1983)

25. J. Y. W. Seto, J. Appl. Phys, **46**, 5247 (1975)

26. D. Ruff et al., J. Non-Cryst. Solids **227-230**, 1011 (1998)

27. J. Kocka et al., Solid State Phenom. **80-81**, 213 (2001)

المنارة للاستشارات

www.manaraa.com

28. N. Wyrsch et al., in Polycrystalline SemiconductorsV. Ed. J. H. Werner, H. P. Strunk, and H. W. Schock, Solid State Phenom. **67-68**, 89 (1999)

29. H. Keppner et al., Appl. Phys. A: Solids Surf. **69**, 169 (1999)

30. S. Veprek, Mat. Res. Soc. Symp. Proc. **164**, 39 (1990)

31. M. Mohri, H.Kakinuma, and T. Tsuruoka, IEICE Trans. Electron. **E-77C**, 1677 (1994)

32. E. Amanatides, D. Mataras, and D. E. Rapakoulias, J. Appl. Phys, **90**, 5799 (2001)

33. H. Fujiwara, M. Kondo, and A. Matsuda, Phys. Rev. B **63**, 115306 (2001)

34. R. E. I. Schropp and M. Zeman, "Amorphous and Microcrystalline Silicon Solar Cells", Kluwer Academic publishers, Dordrecht, p. 60 (1998)

35. J. Koh, Y. Lee, H. Fujiwara, C. R. Wronski, and R. W. Collins, Appl. Phys. Lett. **73**, 1526 (1998)

36. Z. Iqbal and S. Verprek, J. Phys. C **15**, 377 (1982)

المنارة للاستشارات

www.manaraa.com

ACKNOWLEDGEMENTS

The author wishes to express deep appreciation to Dr. Vikram L. Dalal for his invaluable guidance, continuing encouragement and support throughout the course of this research.

The author is also very grateful to committee professors: Dr. Robert J. Weber, and Dr. Douglas K. Finnemore. The priceless debt is to Mr. Max Noack, Ms. Kay Han, Yong Liu, Jason Zhu, Andy Niu, Puneet Sharma, Dr. Gary Tuttle, Dr. Howard Shanks, and Dr. Alan Constant for their countless treasured advice, inspiring discussions and interests towards my work. It was truly my privilege to work with them all at Microelectronics Research Center.

Special thanks are to Ms. Jane Woline at MRC and Ms. Pam Myers at department of Electrical and Computer Engineering for providing cordial accommodation during my years at Iowa State University.

المنارة للاستشارات
www.manaraa.com